



SURFACE CURRENTS OF THE NORTHEAST CHUKCHI SEA

BY

G. L. HUFFORD, B. D. THOMPSON, AND L. D. FARMER

FINAL REPORT

RU - 81

ENVIRONMENTAL ASSESSMENT OF THE ALASKAN CONTINENTAL SHELF

SPONSORED BY

UNITED STATE DEPARTMENT OF INTERIOR
BUREAU OF LAND MANAGEMENT.

APRIL 1977

INTRODUCTION

A knowledge of the surface current patterns along the north Alaskan coast is of both economic and environmental interest. The discovery of oil reserves along the coast has brought development and exploitation on shore with offshore drilling on the continental shelf certain to be undertaken within the next few years. Even the best of planning and the most modern techniques cannot insure that accidental oil spills will not occur. The initial movement of the spilled oil during the summer would be determined primarily by the local surface currents. Thus a working knowledge of the surface currents along the north Alaskan coast is imperative.

During August 1976, a detailed study of the surface currents of the northern Chukchi Sea and western Beaufort Sea coasts was attempted from helicopters from the icebreaker USCGC GLACIER. The objective of this report is to describe the surface circulation during open water.

DESCRIPTION OF STUDY AREA

The investigation was conducted primarily in the region between Icy Cape ($70^{\circ}09'N$, $161^{\circ}55'W$) and Point Barrow ($71^{\circ}20'N$, $156^{\circ}40'W$) and seaward to the pack ice edge. A chart of this study area is shown in Figure 1. A few stations were occupied at Harrison Bay in the Beaufort Sea. (See Figure 9.)

The bathymetry of the Chukchi Sea has been discussed by Creager and McManus (1966). The Chukchi is a continental shelf sea, essentially flat with depths generally $<60m$. The most prominent feature in the northeast Chukchi Sea is Barrow Canyon with depths $>50m$ found as far south as Cape Franklin. The canyon shows a sectional asymmetry, with the steepest side next to the coast.

The most comprehensive analysis of the physical oceanography of the Chukchi Sea to date has been that of Coachman et al (1976). Using data from the cruises of the NORTHWIND (1962), BROWN BEAR (1960), NORTHWIND (1963), GLACIER (1970), and OSHORO MARU (1972), they have based their analysis on two regional water mass groupings, ACW (Alaskan Coast Water) and BSW (Bering Sea Water). In the summer BSW ($1-7^{\circ}C$, $32.2-33.0$ o/oo) dominates the central and western part of the Chukchi Sea. ACW ($2-10^{\circ}C$, <32.2 o/oo) is found in the eastern part of the sea with a recognizable demarcation between it and BSW. The ACW is characterized by lateral gradation from a relatively cold and saline faction on the west, to a warm and less saline faction close to the coast.

The ACW flows north along the Alaskan coast. Near Icy Cape, data from Fleming and Heggarty (1966) show that ACW is often found to spread above a colder, more saline water. They interpreted the cold water to be residual Chukchi Sea winter water.

Current measurements of the surface waters of the Chukchi Sea north of Cape Lisburne are few. The most comprehensive measurements are those from the BROWN BEAR (Fleming and Heggarty, 1966) and the OSHORO MARU (unpublished, 1972). Most of the measurements were of durations of less than one hour. The observations reveal that in the summer surface (0-10m) currents along the Alaskan coast flow northerly parallel to the coast. Speeds of 15 to 25 cm sec⁻¹ are indicated. Near Point Hope there is an acceleration of the flow (~ 40 cm sec⁻¹). Another small acceleration appears to occur near Icy Cape (~ 30 cm sec⁻¹). The few

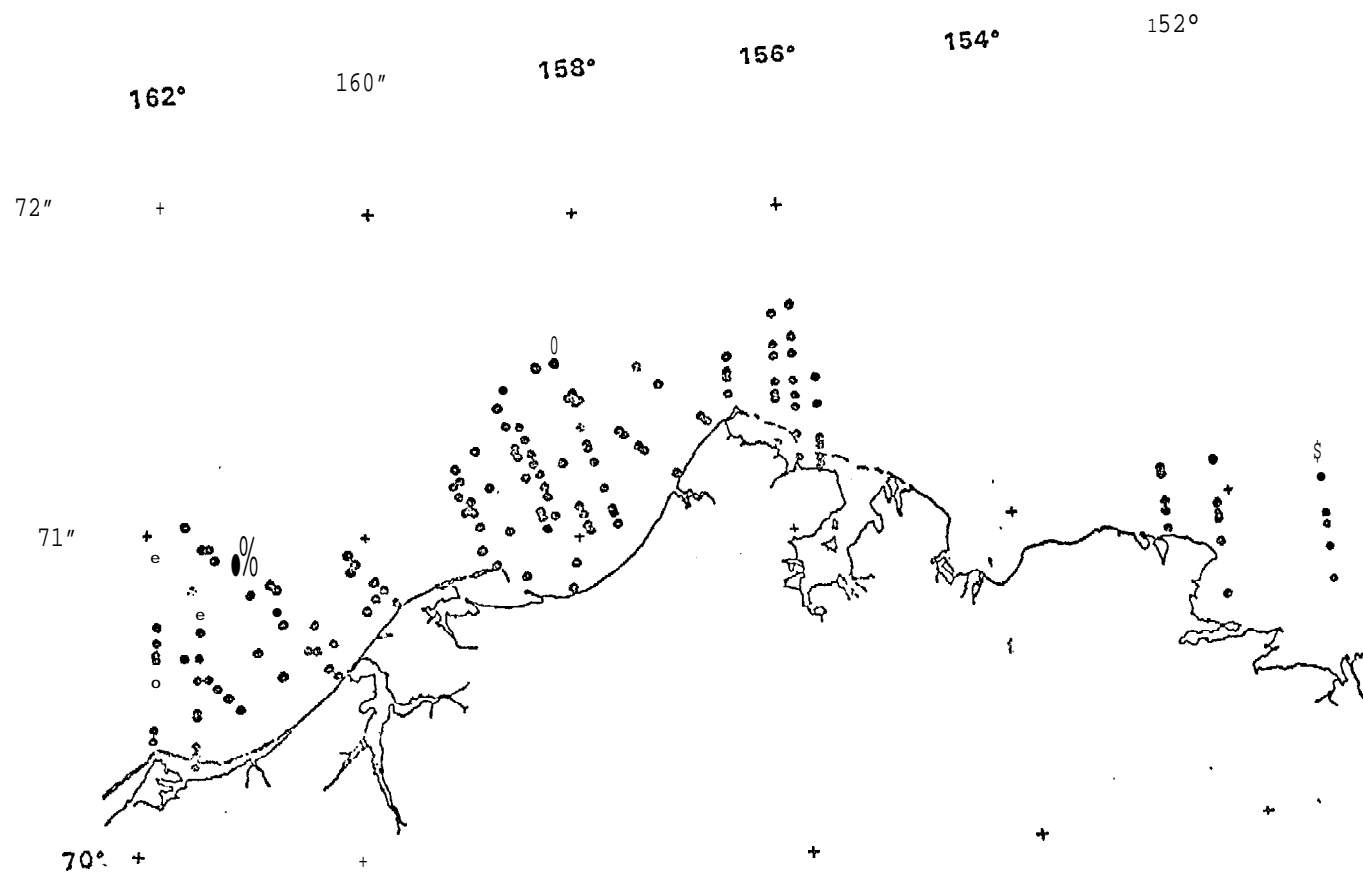


Figure 1. Location of stations taken in the northeast Chukchi Sea and Beaufort Sea.

measurements of currents indicate a considerable complexity and great variability in the flow. Aagaard (1964) reports that offshore of the northeast coast when winds were from the southwest, the surface flow was about 20-50cm sec⁻¹ toward the northeast. When the winds were from the northeast, the surface flow was slowed or reversed.

Wiseman et al. (1974) have examined current flow in the nearshore region of the northeast Chukchi Sea. The currents appeared to be wind driven and severely controlled by bottom topography. The mean velocity of flow for July and August was 21.8cm sec⁻¹ to the north. A small semi-diurnal tidal component was present; the amplitude was only about 1cm sec⁻¹. A major feature of the summer flow was significant reversals in direction associated with changes in wind direction.

No comprehensive picture of the surface water motions in the northeast Chukchi Sea can be obtained from the scattered measurements discussed above. Location of stations have been hampered in the past by the presence of ice. Even in the summer, the polar pack is never far off the coast and can advance onto the shore usually in response to northerly and northwesterly winds. In addition, because of the draft of the icebreakers from which most of the data are obtained, few measurements have been taken shoreward of the 20111 depth contour.

Long-term wind data are available from two locations along the northeast Chukchi Sea coast: Cape Lisburna and Barrow (Figure 2). The predominant summer winds are from the east-northeast and are dominated by the presence of the Polar High centered in the eastern Beaufort Sea (Campbell, 1965). Wind speed rarely exceeds 10m sec⁻¹ in the summer. Southwesterly winds occur about 30 percent of the time and are caused by the passage of low pressure systems. These storms originate in either northern Siberia or the Bering Sea (Klein, 1957). During an average summer, six or seven low pressure systems will pass the region affecting the winds.

Wind stress measurements have been made over Chukchi Sea waters. Results by Walters (1975) indicates the appropriations of a single drag coefficient to describe momentum transfer from the wind to the water. The computed drag coefficient was 1.7×10^{-3} , very similar to the value (1.4×10^{-3}) of Banke and Smith (1971) for the Beaufort Sea coastal waters.

SURFACE CURRENT EXPERIMENT

The surface current study along the northeast Chukchi Sea coast was conducted using air-deployed ESCP (expendable surface current probes). The ESCP, developed by Richardson et al (1972), essentially consists of a plastic tube containing two floats, each with a dye packet, and a timing mechanism which releases the floats once they have reached the bottom of the body of water into which they have been dropped. At a preset time, a red plastic float is released, and later a white plastic float is released. These floats rise under their own buoyancy, and upon surfacing, the floats disperse a bright yellow-green fluorescent dye at the surface. Assuming that the current from the surface to the bottom has not changed during the delay time (~3 minutes) between float releases and that the floats rise at the same rate:

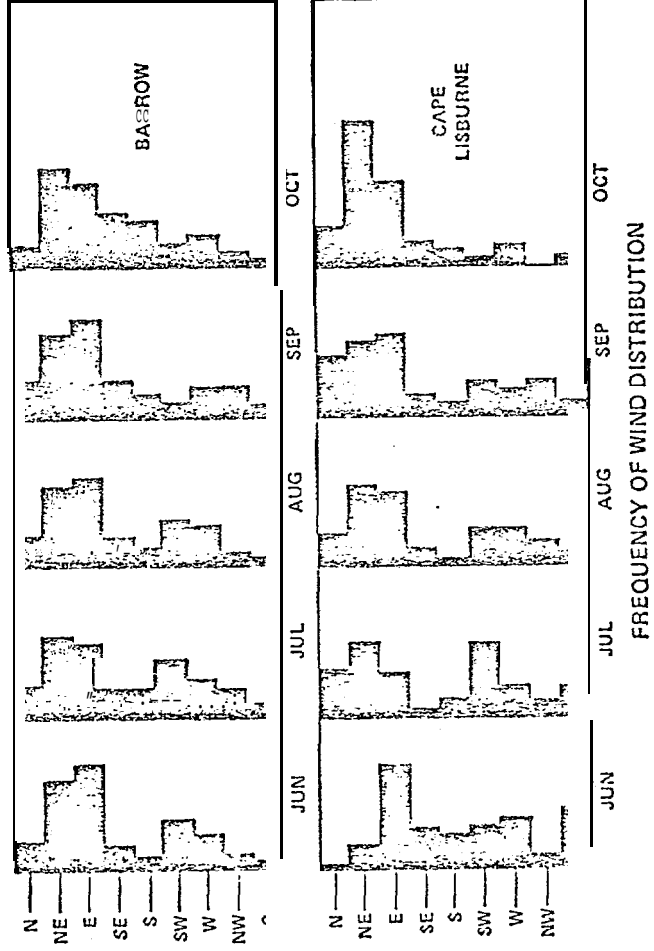
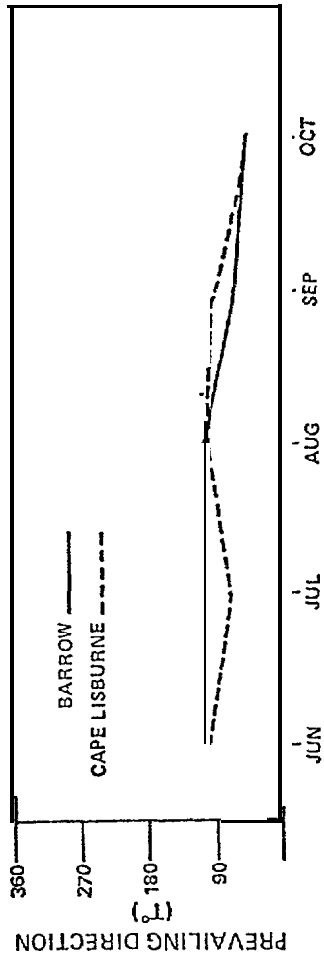


Figure 2. Characteristics of the wind at Barrow and Cape Lisburne, Alaska.

$$\vec{V}_s = \frac{\vec{x}_{RW}}{t_D} \dots \dots \dots (1)$$

where \vec{V}_s is the surface current, \vec{x}_{RW} is the vector separation between the red and white floats, and t_D is the time delay between their releases. The direction of flow is the heading from the white float to the red float.

The ESCP's were launched from an open door of a HH-52 helicopter hovering at 8m above the water. A second helicopter follows at the appropriate time at 300m and photographs the dye marks on the surface. The aerial photographs were obtained with two nadir-viewing, motor-driven, 70mm Hasselblad cameras mounted side by side on a frame mounted in the door of the helicopter. One camera was equipped with ordinary daylight color film. The other camera contained black-and-white film and was equipped with a green filter. A total of 3 to 4 frames were taken at each probe drop station. The helicopter always flew on a heading from white to the red float.

The photographs from each station are screened to determine the one most suitable for further analysis. The chosen photograph is then expanded to 2x for easier removal of the information. A Cartesian coordinate system is superimposed on the photograph and the X and y positions of the floating dye sources are determined. These position locations along with the helicopter's altitude and heading are then used to obtain distance and direction between the two floats. This data along with the time delay (preset) is then used to compute current speed and direction. The accuracy of the reading system for photographs taken at an altitude of 300m is $\pm 2m$. Float separations are typically 75m.

A total of 167 surface current speed-and-direction measurements were collected along the northeast Chukchi Sea coast between 6 and 19 August 1976 (Figure 1). The measurements were taken along transects perpendicular to the coast. Each transect contained 10 stations (unless the pack ice limited the amount of open water). Position of drop stations was determined by using the ship's search radar and vectoring the helicopter to the site. Station locations are probably accurate to $\pm 2km$ offshore and $\pm 0.5km$ inshore.

Climatological data were collected hourly onboard the CGC GLACIER during the entire study. The ship was never more than 37km from the most distant surface current station. Hourly wind data was also obtained from Barrow, Alaska.

During the study, hydrographic stations were occasionally taken for another project (RU #359). That data will be used in this report to determine the hydrography of the region during the current measurement study.

RESULTS

Water Properties

Analysis of the hydrographic data collected for project RU #3.59 agrees with descriptions given for the area. ACW (Alaskan Coast Water), characterized by salinities < 32.0 o/oo, was found from the surface to 20m at those stations

south of Cape Franklin and from surface to 15m at those stations north of Cape Franklin (Figure 3). ACW was found overlying a cold ($<0^{\circ}\text{C}$), saline (>32.0 o/oo) water at all the stations. This cold water is probably residual Chukchi Sea winter water. (See Fleming and Heggarty, 1966.)

The pycnocline between 15 and 20m creates a dynamic barrier to convection affecting the dispersion of any potential oil spill. First it will limit the layer through which the wind drift current can act. Consequently, the wind drift current in time may approach a constant velocity through the entire shallow surface layer (assuming the upper layer is not affected by semi-permanent currents). Second, it will affect the rate and depth of descent of the oil after it has lost its volatile and light fractions.

Winds

Winds observed at Barrow and the CGC GLACIER are shown in Figure 4. There appears to be good agreement between the winds observed at the two stations. As expected, there are small differences in speed and direction. The increased effect of friction over land compared to over sea will cause the wind over land to be slower (this is evident in the record for the period of 7-13 August) and cause a greater deflection in direction.

Three low pressure systems passed through the study area on 8-10, 13-16, and 17-18 August. The winds associated with the systems all showed the same pattern: a shift from easterly winds abruptly to northerly and more gradually to westerly. Wind speed increased as the storms entered the area and decreased as the storm passed by. It must be emphasized that the wind measurements at sea reported here are for a relatively short sampling period during one month only; nevertheless, the winds in the study area offshore appear to correspond closely with the Barrow wind patterns. The minor deviations are probably attributable to the combination of land versus sea location and wide spatial separation between stations.

Currents

Surface current measurements taken during the periods of 8-9, 11-15, 16, 17, and 20 August are shown in Figure 5 through 9. The currents off the coast at Wainwright (Figure 5) show a weak and variable flow ($5\text{-}30\text{cm sec}^{-1}$) toward the northeast. This surface flow is part of the Alaskan Coastal Water. Inshore of the 20m depth contour, the surface flow is opposite in direction to the offshore currents. Speeds of 5 to 24cm sec^{-1} were observed. The 8-9 August period was dominated by easterly to northeasterly winds with these components having a mean speed of 8.9m sec^{-1} . It should be noted that the winds were predominantly westerly from 3-7 August. The currents in Figure 5 probably represent a transient state. According to Ekman (1905), a wind-driven current in shallow water near a coast should reach steady state within 1 or 2 pendulum days.

Three transects were occupied on 11 August off Icy Cape (Figure 6). The interesting feature is the anticyclonic gyre located inshore of the ACW flow and in the lee of Icy Cape. The diameter of the gyre is estimated at 20km. In the southern Chukchi Sea an anticyclonic eddy has been observed in the lee

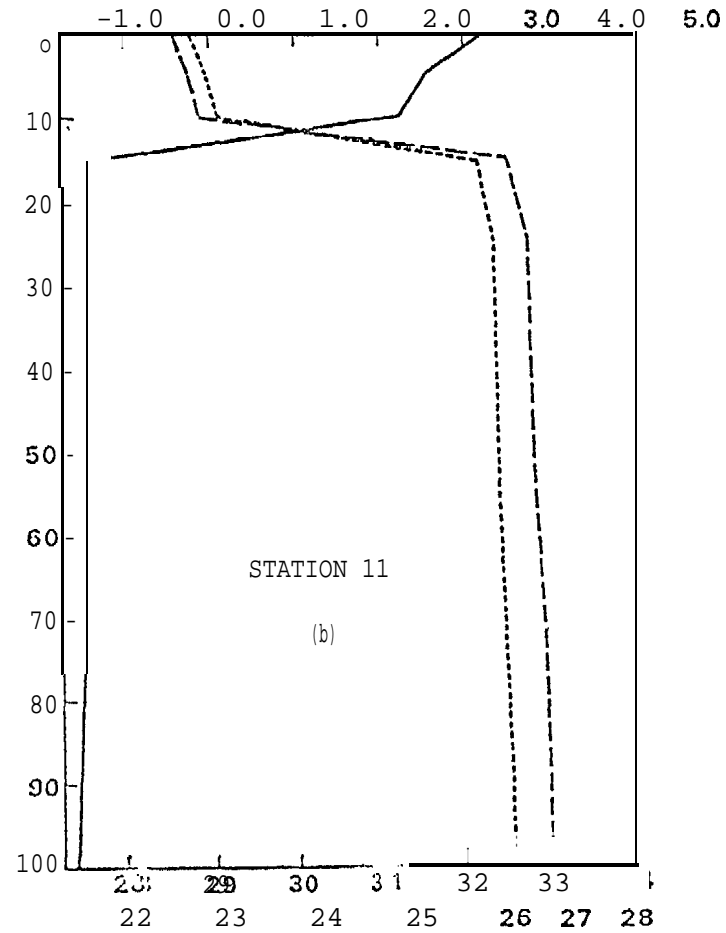
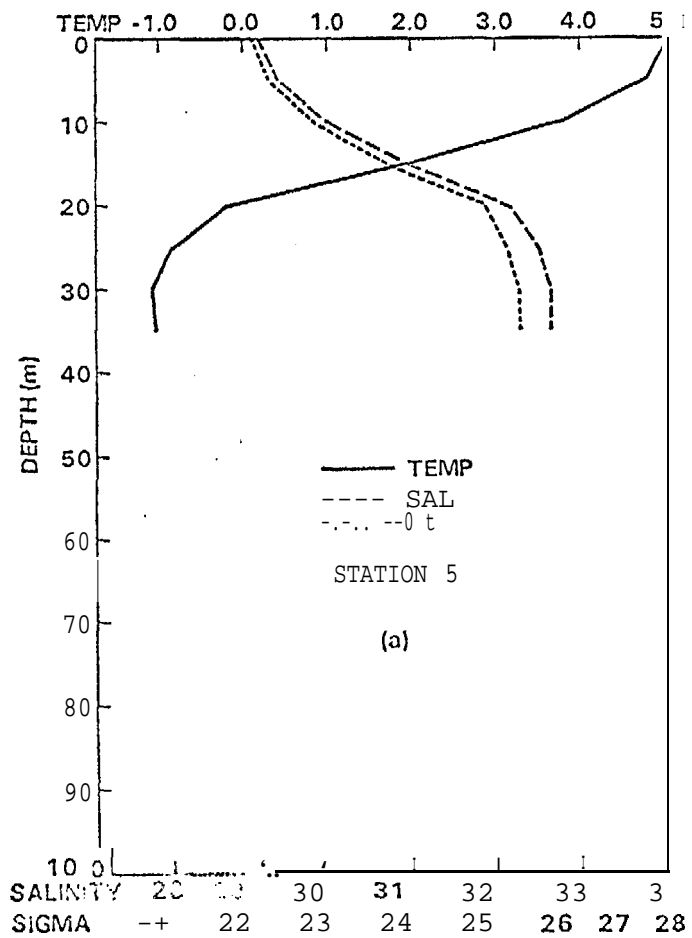


Figure 3. Temperature, salinity and sigma-t of stations 5 and 11.

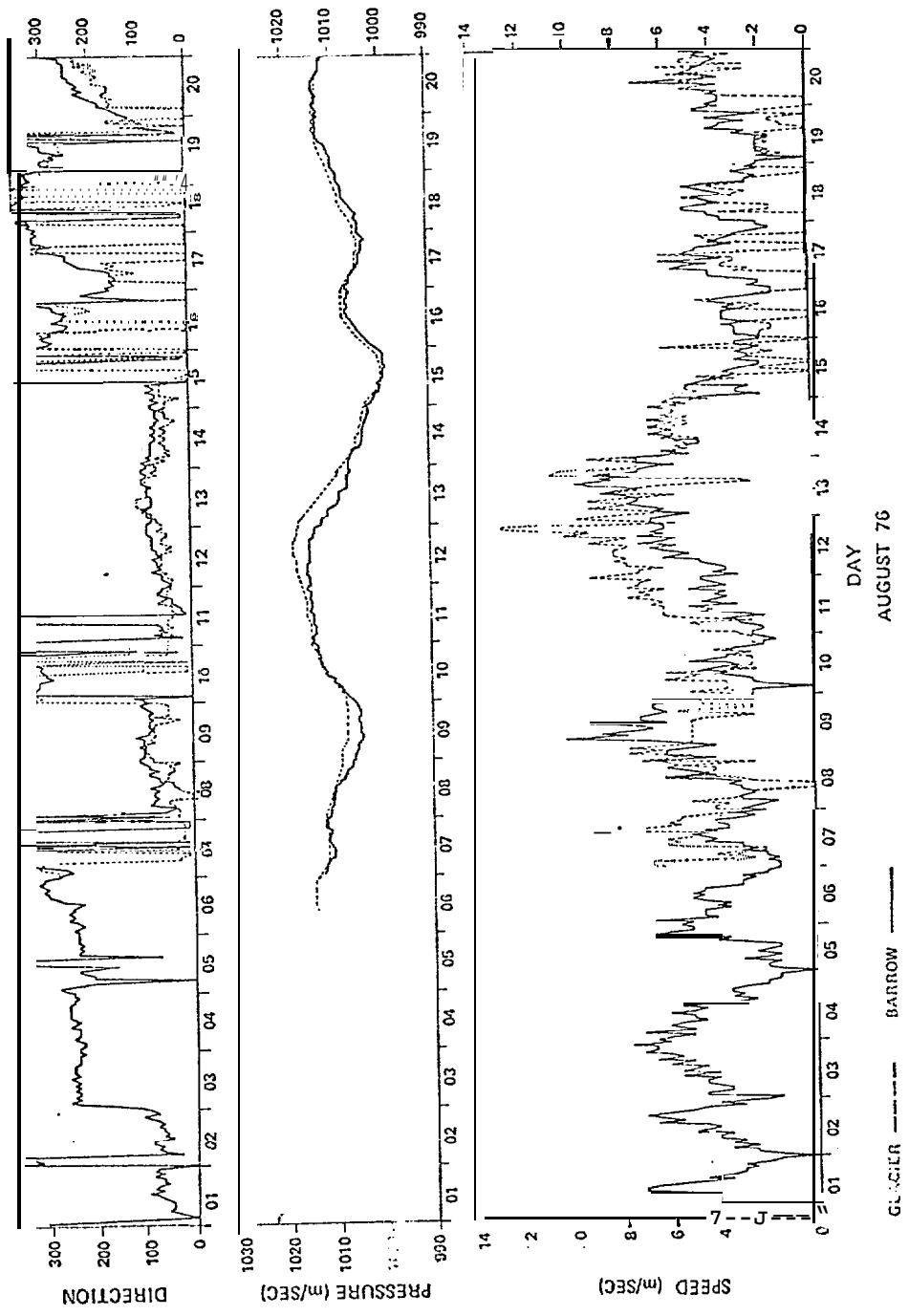


Figure 4. Winds observed at Barrow and the CCC GLACIER, August, 1976.

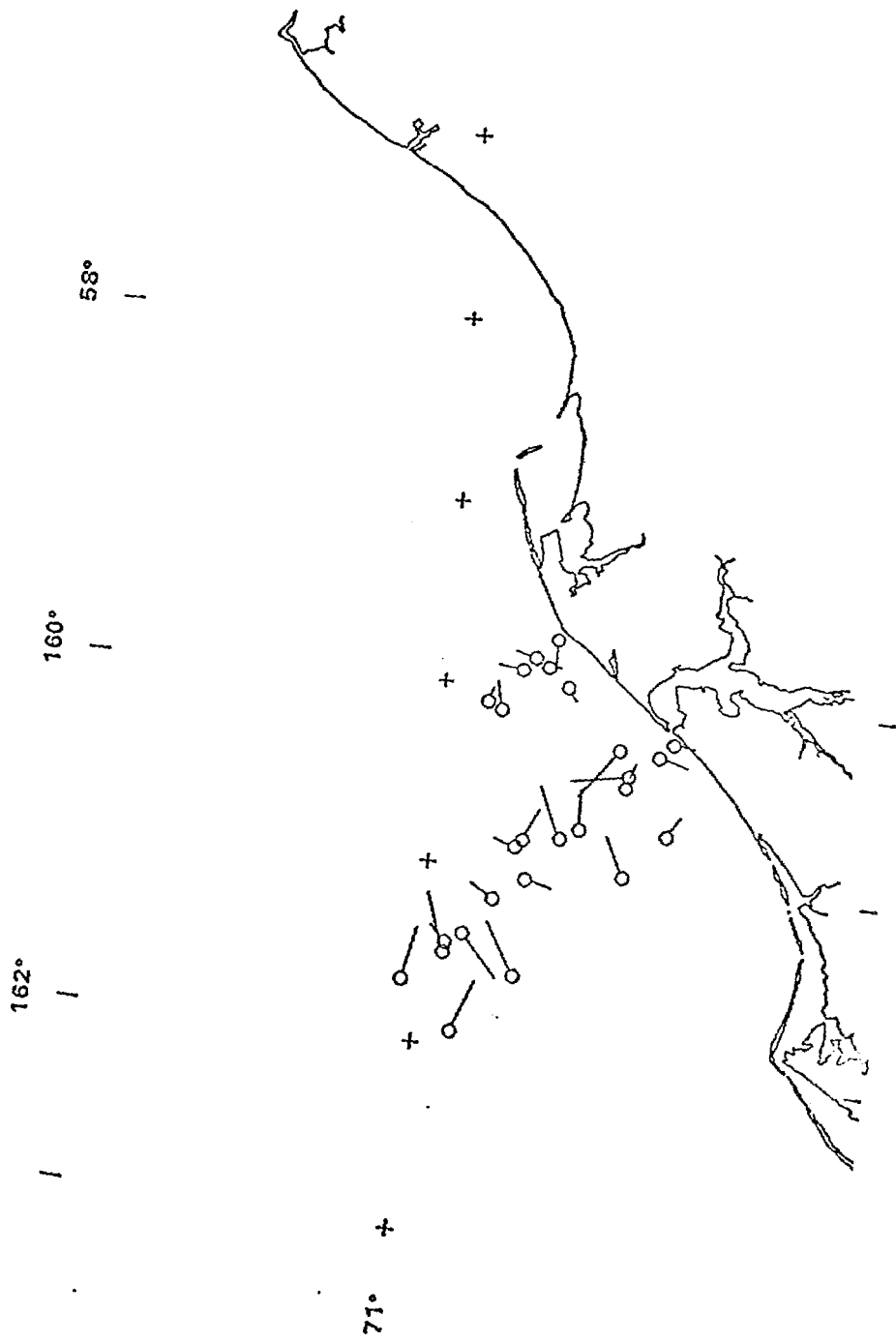


Figure 5. Surface currents off the Chukchi Sea coast at Wainwright, Alaska, 8-9 August 1976.

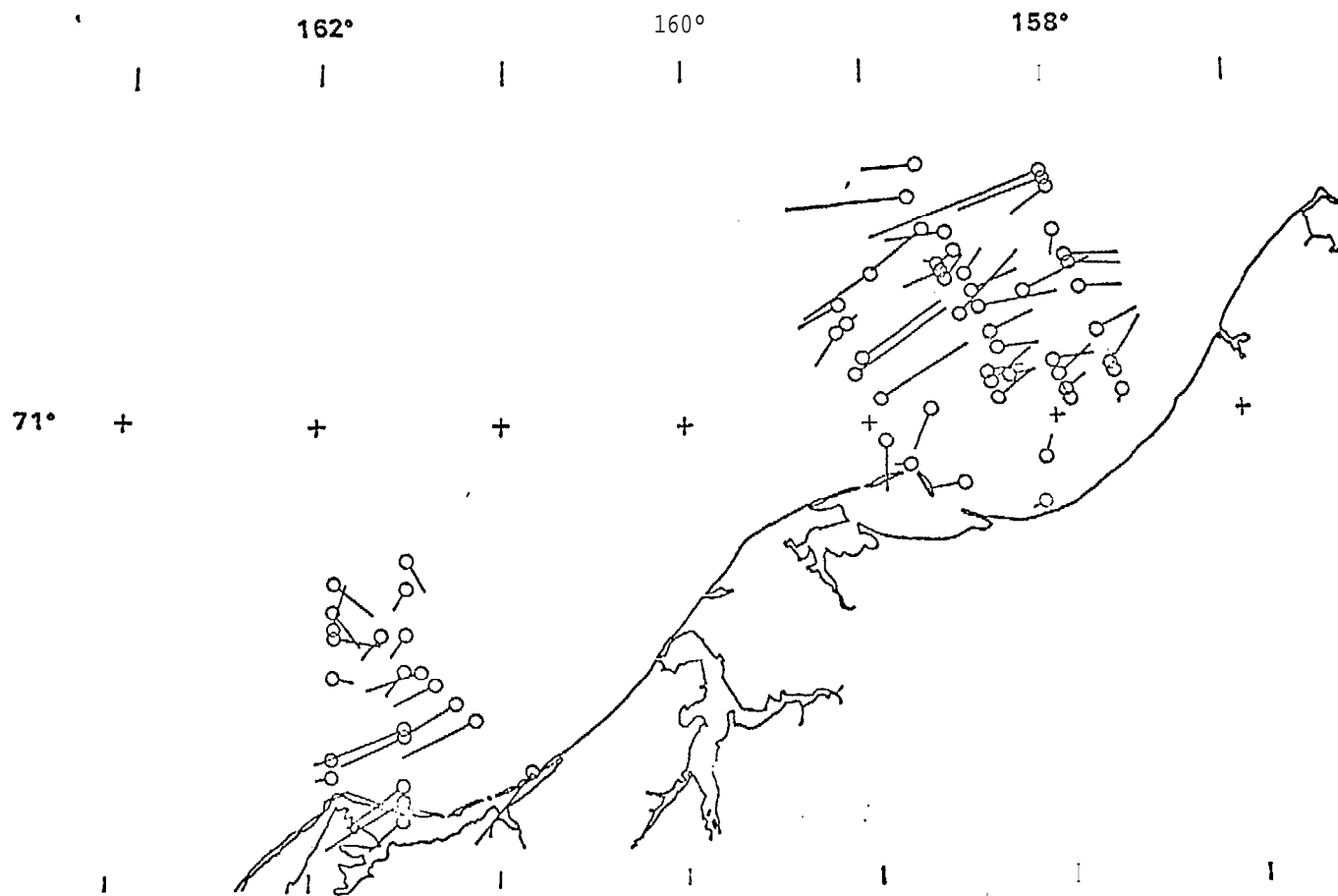


Figure 6. Surface currents off the Chukchi Sea coast from Icy Cape to Peard Bay,
" 11-15 August 1976.

of the Point Hope-Cape Lisburne peninsula (Ingham and Rutland, 1971). Thus it is not surprising that an eddy should be found in the lee of Icy Cape. However, this is the first documentation of this feature.

The major feature of the surface currents observed off Peard Bay (Figure 6) is a three "banded" current regime: a southerly flow inshore and offshore separated by a northeasterly flow. Previous evidence of the southerly flow offshore only 70km from the coast does not exist in the literature. Speeds of 30 to 71cm sec⁻¹ were measured. There appears to be a general acceleration of the northeasterly flow (to ~55cm sec⁻¹) near Cape Franklin.

The currents measured off of Point Barrow on 16 August (Figure 7) show the ACW flow to be found close to shore and to exhibit an acceleration in speed. The currents just east of Point Barrow and near shore appear to be wind driven. The winds on 16 August were predominantly westerly. Current direction was to the northeast. Those stations were nearly reoccupied on 17 August (Figure 8) when the predominant winds were southeasterly. The current direction was to the northwest.

Three transects were occupied near Cape Halkett in the Beaufort Sea on 20 August (Figure 9). Wind direction was predominantly southeasterly. The currents show a flow offshore. The currents in the southern end of Harrison Bay appear to be controlled by bottom topography. Current speeds (3-27cm sec⁻¹) and direction suggest the surface flow is wind driven.

DISCUSSION

A study of the surface currents along the northeast Chukchi Sea coast in August 1976 shows that the flow is dominated by the northeasterly flow of ACW.³ This relatively warm current has its source in the Bering Strait (Coachman et al, 1976). This warm coastal current is close to the coast and narrow. It is as narrow as 25-40km in places and even narrower (~20km) near Point Barrow. The highest current speeds were observed near Cape Franklin and Point Barrow. The current seems constrained to follow bottom contours. Once the warm coastal current reaches Point Barrow, the current turns sharply to the right 40km north-east of Point Barrow again following the bottom contours.

It is interesting to note that northeasterly winds during the study period (3 to 10m sec⁻¹) were not intense enough to cause current reversal of the warm coastal current. On 8-9 August during northeasterly winds (mean of 8.9m sec⁻¹), the surface flow was reduced in speed and variable in direction, but did not reverse.

During periods of easterly-northeasterly winds, nearshore currents were found to flow towards the south parallel to the bottom topography, as one would expect from Ekman dynamics (Ekman, 1905). During westerly winds the nearshore currents were northerly just south of Barrow. A scatter diagram for wind speed versus current speed is shown in Figure 10. The linear correlation between wind and current speed yields a correlation coefficient of +0.77 at the 0.95 confidence level. The relationship is of greater significance than is indicated by the numerical coefficient, since the effects of time lags in the response of the currents to changes in the wind regime are not taken into account.

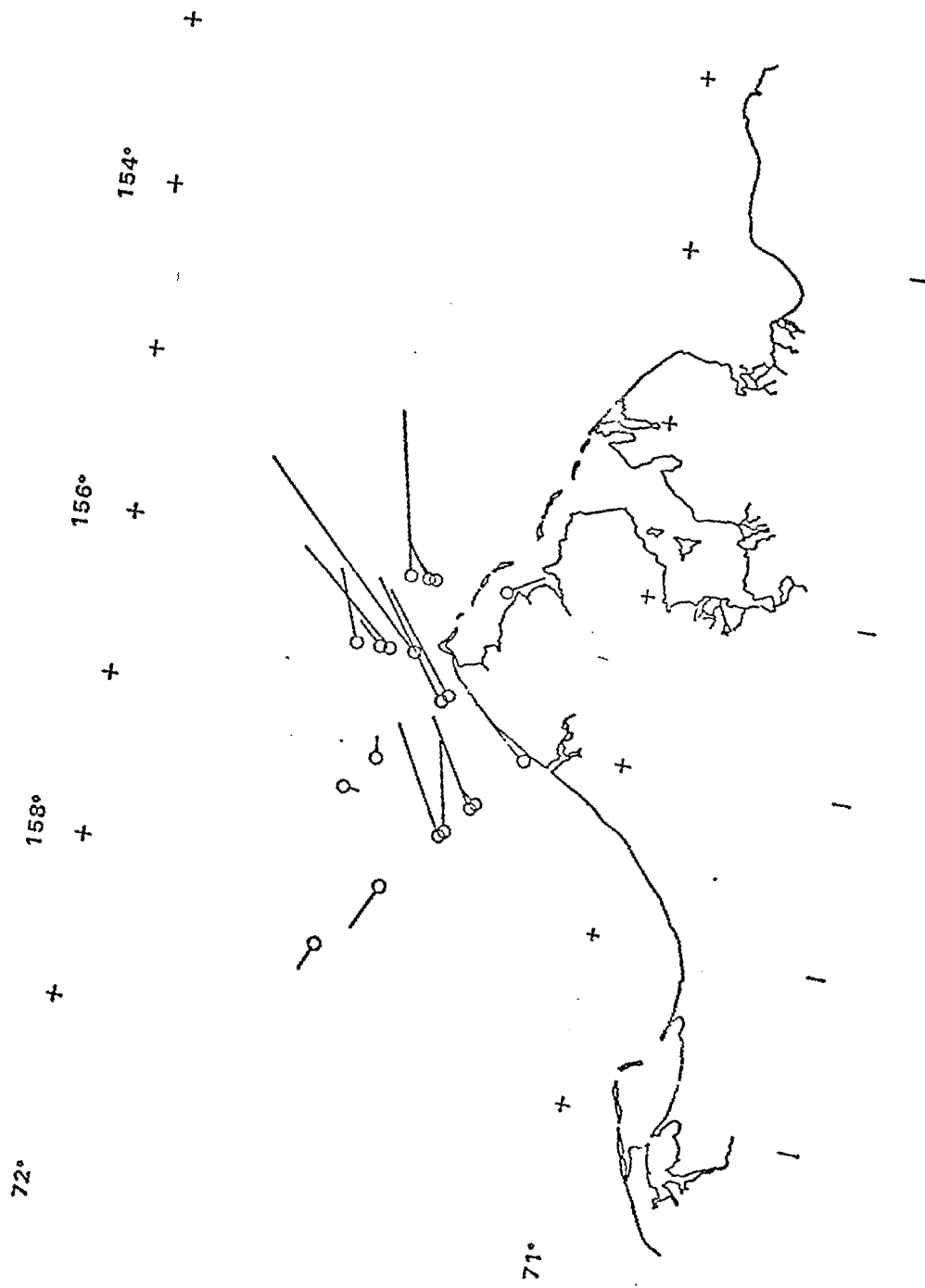


Figure 7. Surface currents off Point Barrow, 16 August 1976.

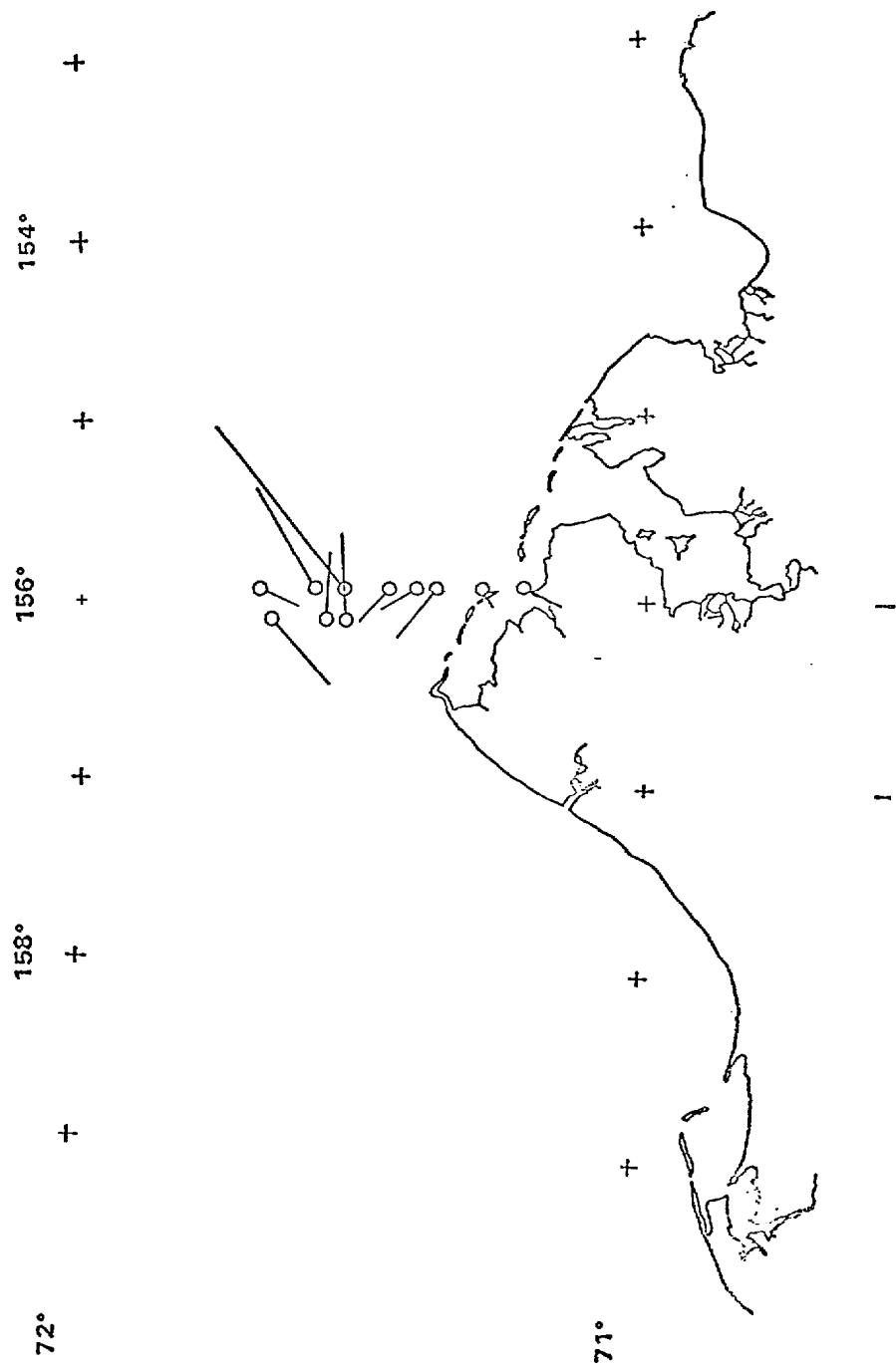


Figure 3. Surface currents off Point Barrow, 17 August 1976.

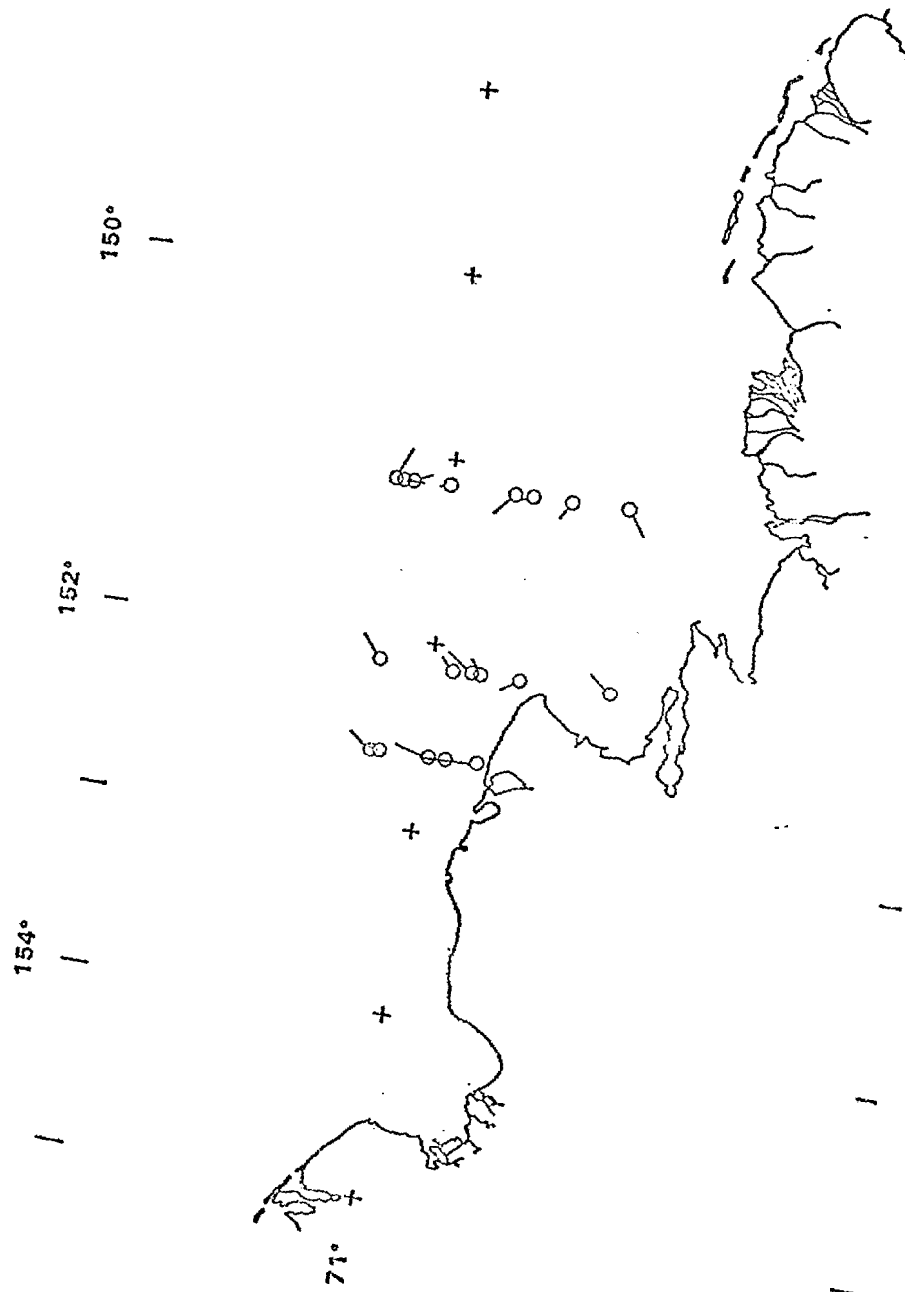


Figure 9. Surface currents of Barrington Bay, 20 August 1976

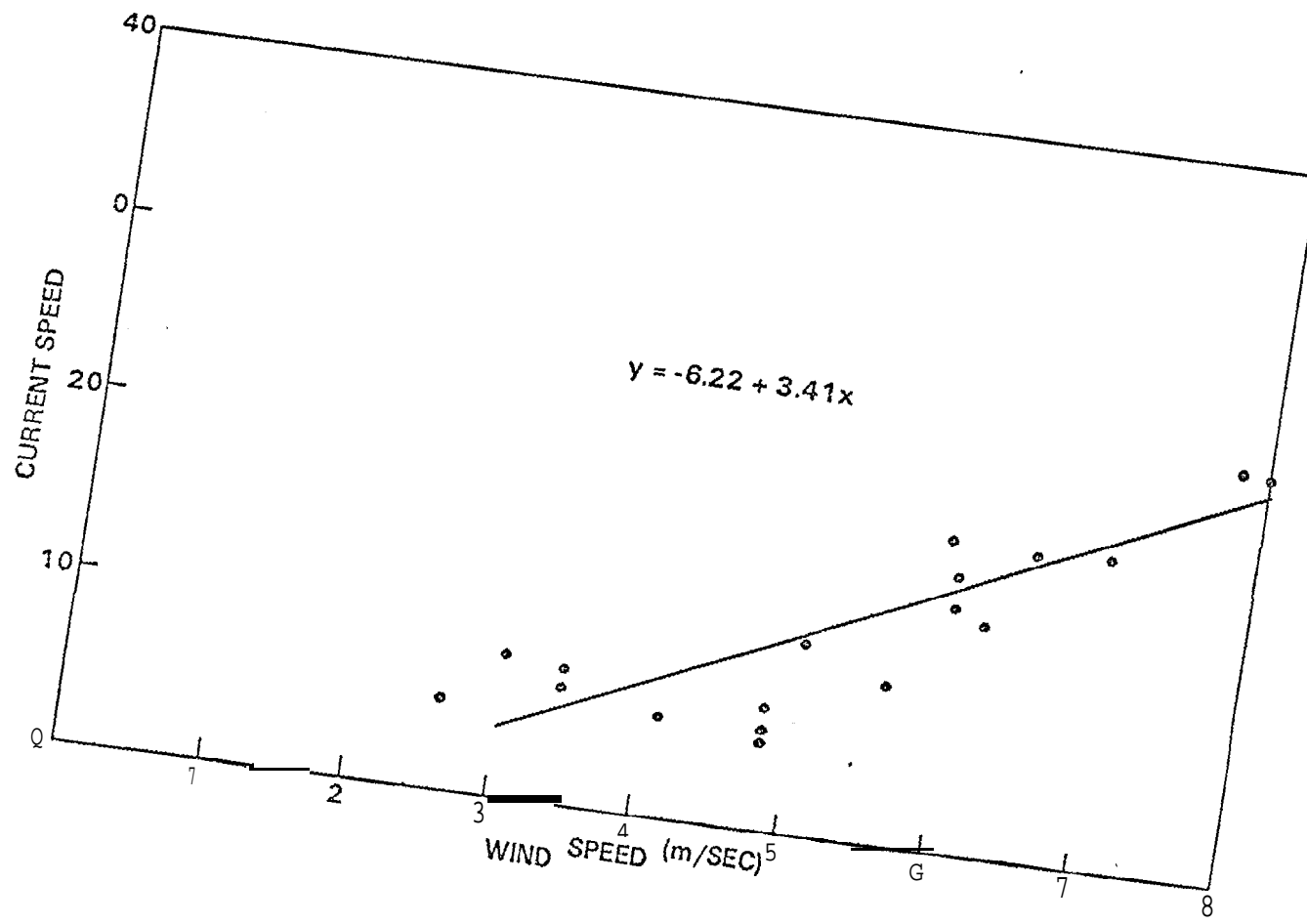


Figure 10. Scatter diagram of wind speed versus current speed for the northeast Chukchi Sea.

A scatter diagram for wind speed versus current speed for the surface currents of eastern Harrison Bay is shown in Figure 11. It should be mentioned that this diagram only represents the relationship of the currents to the wind when the winds are from the south. Although there is an obvious qualitative correlation between high wind speed and high current speed, the data do not justify any attempt to fit a curve through the sample points.

Analysis of the surface currents inside the 18m depth contour taken in August 1976 in the Chukchi Sea show a southerly flow under the influence of the prevailing easterly-northeasterly winds and that this flow is reversed with little observable time lag when the wind is from the southwest or west. The statistical correlation between wind and water movement gives a means for predicting the rate of movement of pollutants released into this arctic coastal environment.

The southwesterly surface current flow seaward of the warm northeasterly flow has not been described in the literature. Current speeds greater than 70 cm sec^{-1} were measured indicating that the wind is not the primary driving force. There is no way to determine from this data whether the current is a semi-permanent or a transient feature. There is some circumstantial evidence that the southerly flow occurs in May and June. Drifter buoys released into the ice as part of the AIDJEX ice drift studies were found to drift from the Beaufort Sea south into the Chukchi Sea and then reverse back to the northwest in late June and early July (Bob Pritchard, personal communication).

The importance of this southerly flow is that if oil moving offshore or a spill were to occur offshore, oil could become entrained into the current and be carried south rather than north as the surface currents closer to shore might suggest.

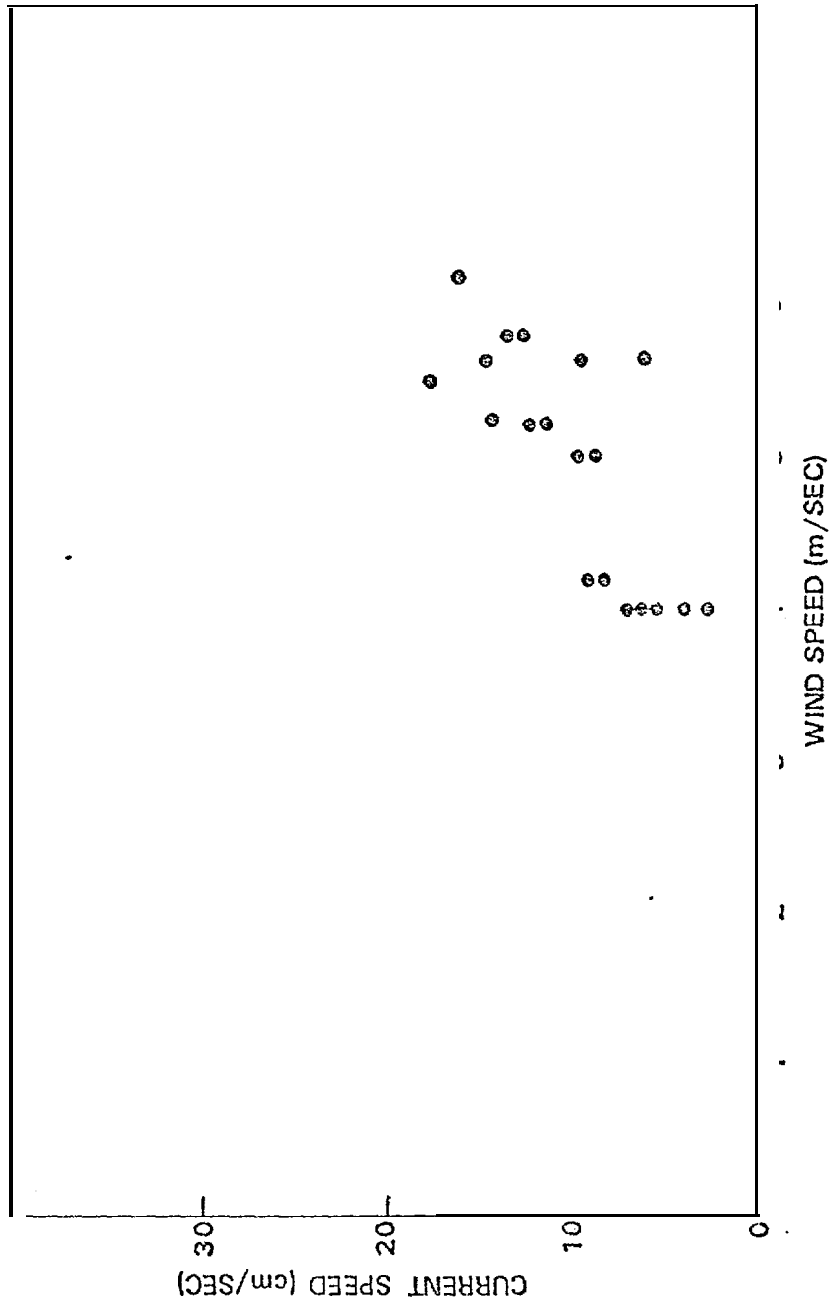
Transport per unit width of the water column ($\text{m}^2 \text{ sec}^{-1}$) was calculated for the transects off Peard Bay (Figure 6) to examine in more detail the three "banded" current (Figure 12). The two southerly current regimes are quite evident indicating that the flow also occurs at depth. Mass transport was calculated (Table 1) for each section. The totals shows that the offshore southerly flow dominated. The transport (Sv) for the area is shown in Figure 13.

This should not be treated as representative of the transport for this area. We know that transports through the system can vary by a few tenths of a Severdrup in one or two days (Couchman et al., 1976). However, the calculations do give some quantitative aspects of the passage of this offshore water to the south.

TABLE 1

TRANSPORT (Sv; + = north) THROUGH SECTIONS OFF PEARD BAY
(STATION NUMBERS FROM APPENDIX)

<u>NEARSHORE FLOW</u>	<u>COASTAL CURRENT</u>	<u>OFFSHORE FLOW</u>
-0.1	0.2	-0.6



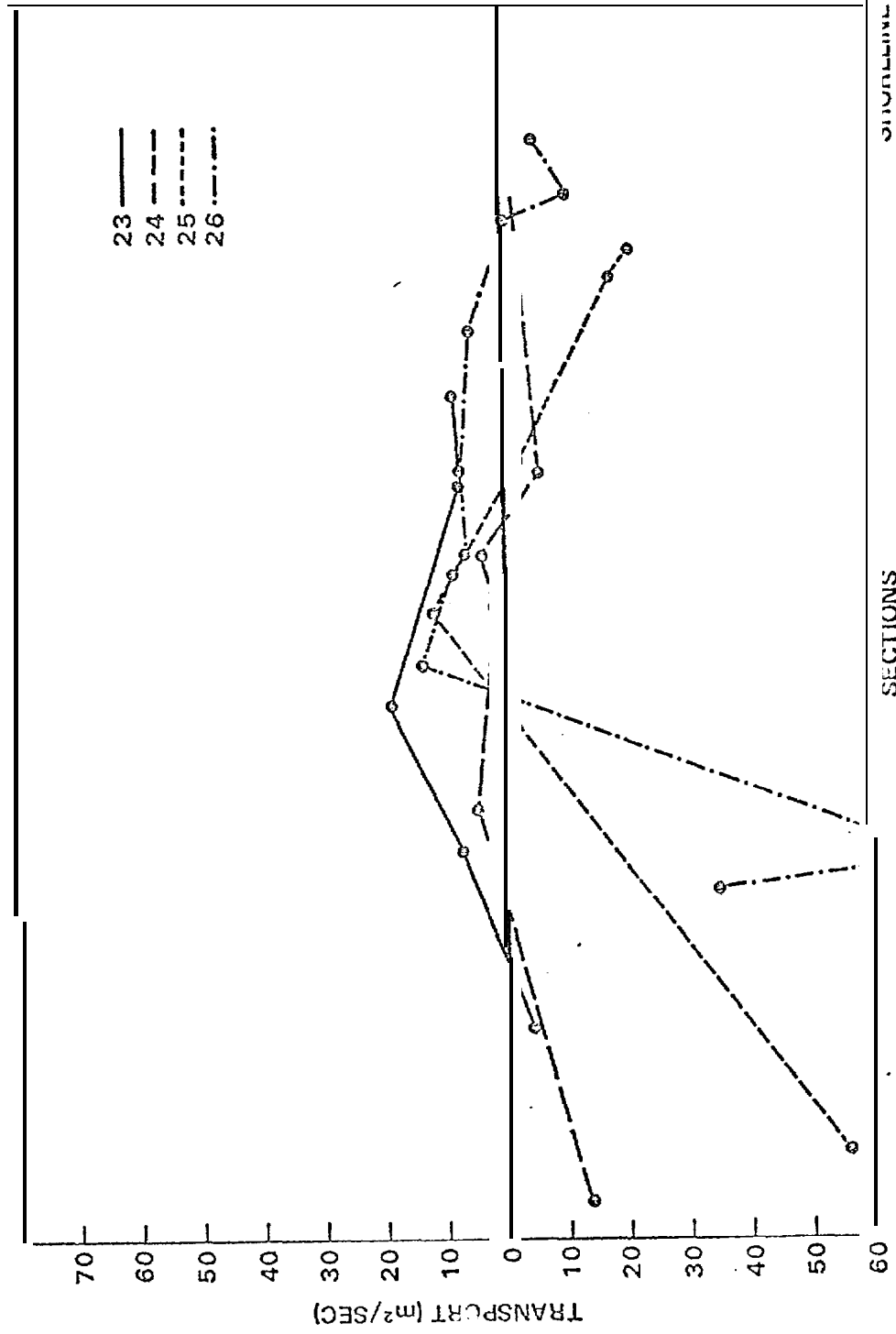


Figure 12. Transport ($m^2 \text{ sec}^{-1}$) for sections off Peard Bay (see appendix for station location).

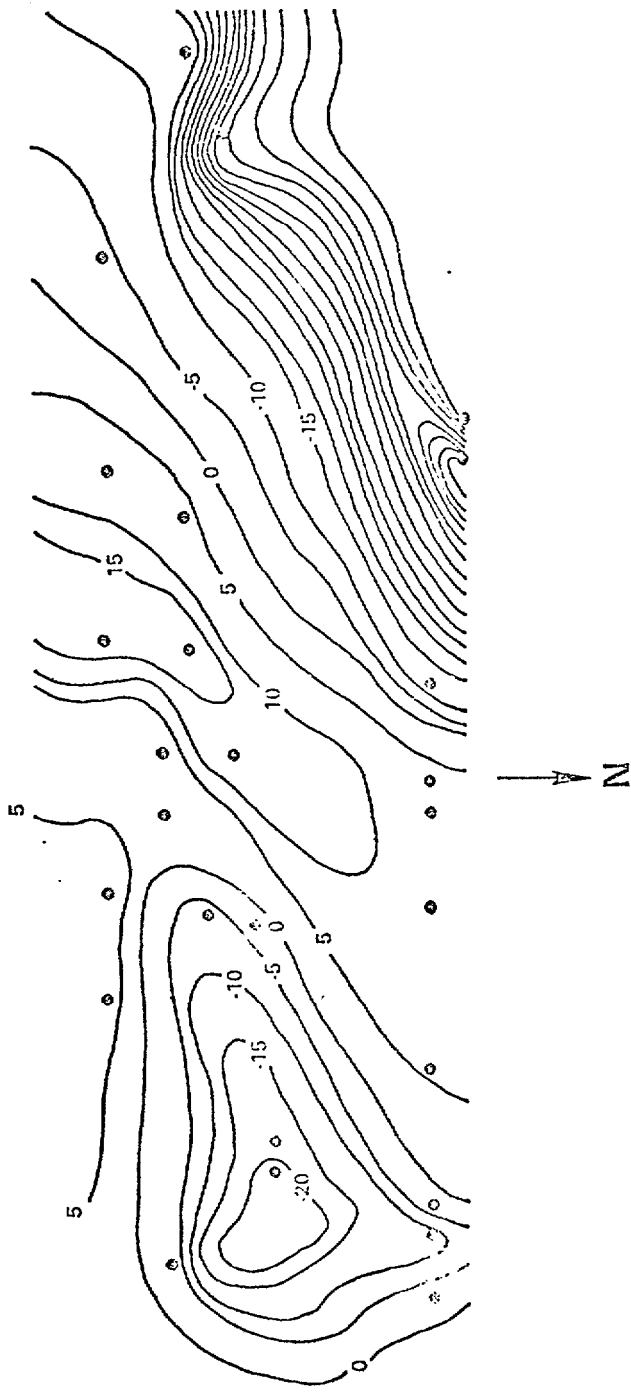


Figure 43 Transport plotted for the sections off Peard Bay.

SUMMARY

Our knowledge of the surface currents of the northeast Chukchi Sea is quite inadequate for forecasting the flow. This stems largely from the lack of a dedicated oceanographic program to the area. Because of this lack of knowledge, only a descriptive approach can be taken for presenting the observed conditions rather than an analytical approach to understand processes.

The dominant surface flow in the northeast Chukchi Sea is the warm coastal current which originates in the Bering Strait and flows toward the northeast turning to the right into the Beaufort Sea northeast of Point Barrow. This current can be classified as a semi-permanent flow showing slowing and sometimes reversal for short periods especially during northeast winds.

An anticyclonic eddy has been observed in the lee of Icy Cape. The importance of this feature is that it can be a "trap" for oil spilled on the area. More data is needed to determine if this eddy is a semi-permanent feature like the eddy in the lee of Point Hope-Cape Lisburne.

Nearshore currents along the northeast Chukchi Sea coast are wind driven and show a southwesterly flow under the influence of easterly-northeasterly winds and northeasterly flow during westerly-southwesterly flow. Analysis of these nearshore currents with the winds produced a means of predicting the rate of movement of oil spilled into this area. This means of predicting local wind drift current patterns should have considerable utility until more precise knowledge of the coastal currents is available.

The southwesterly current observed 70km off the Alaskan coast is an unknown feature. Current data presented by Coachman et al (1976) suggest southerly flow in the north central region of the Chukchi Sea near 164°W. There is no evidence to indicate that the flow in the central part of the sea has shifted closer to the Alaskan coast. Future study of this southwesterly flowing current is necessary to determine the processes affecting the flow.

REFERENCES

- Aagaard, K. . Features of the Physical Oceanography of the Chukchi Sea in the Autumn. Univ. Washington Department, Oceanography, M.S. thesis, 41 pp. (1964) .
- Banke, E. G. and Smith, S. D. Wind Stress Over Ice and Over Water in the Beaufort Sea. Journal of Geophysical Research, 76:7368-7374 (1971).
- Campbell, W. J. The Wind Driven Circulation of Ice and Water in a Polar Ocean. Journal of Geophysical Research, 70:3279-3301 (1965).
- Coachman, L. K. Aagaard, K., and Tripp, R. B. Bering Strait: The Regional Physical Oceanography. University of Washington Press, Seattle, Washington, 172 pp. (1976).
- Creager, J. S. and McManus, D. A. Geology of the Southeastern Chukchi Sea. Environment of the Cape Thompson Region, Alaska. U.S. Atomic Energy Commission Report, Division of Technical Information (1966).
- Ekman, V. W. On the Influence of the Earth's Radiation on Ocean Currents. Ark. f. Mat. Astron. och Fysik, 2(11):1-53 (1905).
- Fleming, R. H. and Heggarty, D. Oceanography of The Southeastern Chukchi Sea. Environment of The Cape Thompson Reg Alaska. U. S. Atomic Energy Commission Report, Division of Technical Information (1966).
- Ingham, M. c. and Rutland, B. A. Physical Oceanography of the Eastern Chukchi S22 Off Cape Lisburne-Icy Cape. WEBSEC 70, An Ecological Survey in the Eastern Chukchi Sea, September-October 1970. U. S. Coast Guard Oceanographic Report No. 50, 206 pp. (1971).
- Klein, W. H. Principal Tracks and Mean Frequencies of Cyclones and Anticyclones in the Northern Hemisphere. Weather Bureau Research Paper No. 40, Washington, DC (1957).
- Walters, C. D. Drag Coefficient and Roughness Length Determinations on an Alaskan Arctic Coast During Summer. Boundary-Layer Meteorology 8:235-237 (1975) .
- Wiseman, W. J. Suhayda, J. N., Hsu, S. A., and Walters, C. D. Characteristics of Nearshore Oceanographic Environment of Arctic Alaska. The Coast and Shelf of the Beaufort Sea, Arctic Inst. North Am., Arlington, VA (1974).

APPENDIX

Position

Tr. ID.	Latitude	Longitude	Date	Time	Speed (cm/sec)	Heading (°T)
5A	70°47.7'	159°43.1'	8 Aug	1545	13.0	267°
5B	70°49.7'	159°49.4'	8 Aug	1547	9.3	017°
5C	70°51.1'	159°54.1'	8 Aug		11.8	008°
5D	70°54.2'	160°5.1'	8 Aug		5.8	111°
5E	70°35.2'	160°8.1'	8 Aug			
63	70°53.2'	160°9.0'	8 Aug	1417	14.6	079°
6A	70°48.4'	159°52.4'	8 Aug		3.8	178°
7A	70°46.1'	159°58.3'	8 Aug		5.6	231°
8A	70°40.3'	160°17.8'	9 Aug	0956	35.7	306°
8 C	70°43.7'	160°27.9'	9 Aug	1024		
8E	70°50.4'	160°52.8'	9 Aug	1040	18.0	115°
8F	70°51.6'	160°55.5'	9 Aug	1048	8.3	020°
8G	70°53.7'	161°2.4'	9 Aug	1054		
8H	70°54.9'	161°6.60	9 Aug	1101		
8B	70°39.4'	160°27.5'	9 Aug	1337	32.6	350°
9D	70°45.4'	160°48.7'	9 Aug	1410	30.3	066°
9G	70°57.2'	161°28.1'	9 Aug	1457	12.6	032°
9H	70°59.6'	161°36.9'	9 Aug	1503	9.5	048°
9A	70°34.6'	160°15.7'	9 Aug	1648	9.0	190°
9B	70°35.7'	160°19.8'	9 Aug	1655	15.6	196°
9C	70°39.0'	160°31.1'	9 Aug	1658	13.3	110°
9F	70°43.5'	160°47.6'	9 Aug	1718	21.1	089°
9G	70°48.6'	161°5.3'	9 Aug	1635	12.8	194°
9J	70°54.7'	161°25.3'	9 Aug	1758	31.3	228°
9K	70°56.8'	161°32.9'	9 Aug	1-807	33.9	071°
9K	71°1.1'	161°42.0'	9 Aug	1-820	29.6	102°

Position

St. ID.	Latitude	Longitude	Date	Time	Speed (cm/sec)	Heading (°T)
1K	70°54.3'	161°42.5'	9 Aug	830	30.7	111°
1J	70°48.4'	161°34.6'	9 Aug	838	33.1	060°
1B	70°33.6'	160°45.2'	10 Aug	928	11.9	122°
1C	70°38.3'	161°0.6'	10 Aug	945	23.6	064°
9A	70°23.2'	161°49.4'	11 Aug	1925	6.61	259°
9B	70°25.5'	161°49.4'	11 Aug	935	7.82	253°
9D	70°34.3'	161°49.4' "	11 Aug	956	9.81 -	103°
9E	70°37.8'	161°49.4'	11 Aug	017	25.0	099°
9F	70°38.8'	161°49.4'	11 Aug	025	24.6	016°
9G	70°33.6'	161°49.4' "	11 Aug	030	22.1	143°
9H	70°44.4'	161°49.4'	11 Aug	040	26.7	128°
18B	70°16.4'	161°26.1'	11 Aug	403	23.3	228°
18C	70°24.0'	161°26.1'	11 Aug	408	52.9	238°
18D	70°21.6'	161°26.1' -	11 Aug	416	39.4	233°
18E	70°25.6'	161°26.1'	11 Aug	422	40.0	245°
18F	70°26.8'	161°26.1'	11 Aug	427	53.3	248°
18G	70°32.7'	161°26.1'	11 Aug	443	14.4	217°
18H	70°36.9'	161°26.1'	11 Aug	448	12.0	213°
18J	70°41.7'	161°26.1'	11 Aug	458	11.1	210°
18K	70°44.3'	161°26.1'	11 Aug	505	17.4	150°
15A	70°22.3'	160°50.2'	11 Aug	645	13.0	217°
15B	70°27.4'	161°6.7'	11 Aug	655	16.6	243°
15C	70°29.7'	161°14.6'	11 Aug	706	15.5 "	238°
15D	70°31.5'	161°20.7'	11 Aug	718 "	14.2	243°
15E	70°32.8'	161°25.5'	11 Aug	731	11.9	251°
15F	70°36.5'	161°37.2'	11 Aug	742	3.0	217°

Position

Point	Latitude	Longitude	Date	Time	Speed (knots)	Heading (°T)
20D	71°9.3'	159°8.0'	14 Aug	1642	19.2	214°
20C	71°7.3'	159°5.8'	14 Aug	1658		
20B	71°4.7'	159°3.1'	14 Aug	1704	64.7	056°
20A	70°57.0'	158°54.9'	14 Aug	1711	27.0	082°
21A	70°55.0'	158°43.1'	14 Aug	1726	7.4	267°
21A	70°55.0'	158°43.1'	14 Aug	1730	5.0	267° "
21C	71°2.9'	153°49.2'	14 Aug	1743	58.8	0610
21C	71°2.9'	158°49.2'	14 Aug	1745	60.0	058°
21D	71°5.7'	158°50.9'	14 Aug	1750		Failure
21E	71°7.6'	158°52.3'	14 Aug	1804	55.9	05.6°
21F			14 Aug			
21G	71°13.6'	158°56.9'	14 Aug	1320	14.5	242°
21G	71°16.2'	158°46.4'	14 Aug	2050	44.5	236°
22E	71°10.8'	158°42.0'	14 Aug	2108	"	
22D	71°1.4'	158°35.1'	14 Aug	2120	23.7	204°
22C	70°53.0'	158°28.2'	14 Aug	2131	17.5	262°
23G	71°16.6'	158°25.1'	14 Aug		20.0	249°
23A	70°50.6'	158°5.1'	14 Aug	2201	5.4	242°
23B	71°2.3'	158°13.7'	15 Aug	1040	24.9	052°
23C	71°4.1'	158°15.1'		1046	28.1	050°
23D	71°5.5'	158°16.3'		1056	18.7	0810
23E	71°11.6'	158°21.1'		1145	18.1	044°
23F	71°13.7'	158°23.9'		1200	14.0	036°
23	71°17.7'	158°26.0'		1206	3.9	284°
23J	71°21.2'	158°28.9'		1223	36.6	282°
23K	71°24.6'	158°31.4'	15 Aug	1233	70.4	266°

Position

St. I.D.	Latitude	Longitude	Date	Time	Speed (cm/sec)	Heading (°T)
5K	71°26.9'	158°27.4'	15 Aug	1239	50.7	154°
5K	71°29.6'	158°27.1'		1242	28.0	267°
5L/2	71°21.9'	158°21.4'		1301	32.4	264°
5L/25H	71°21.1'	158°20.3'		1309	11.2	226°
5M	71°16.3'	158°17.3'		1325	14.1	036°
5N	71°14.5'	158°15.7'		1528	26.1	068°
5O	71°12.8'	158°14.4'		1535	4.4	081°
5P	71°10.1'	158°12.6'		1541	15.1	066°
5Q	71°7.7'	158°10.8'		1550	10.5	085°
5R	71°4.8'	158°8.3'		1558	0.6	079°
5S	70°55.3'	158°1.8'		1606	8.2	197°
5T	71°1.4'	157°54.9'		1629	7.1	332°
5U	71°2.3'	157°56.0'		1631	1.1	052°
5V	71°4.2'	157°58.1'		1634	1.8	048°
5W	71°8.3'	158°3.5'		1644	1.4	084°
5X	71°12.9'	158°9.1'			0.7	065°
5Y	71°1.6'	157°39.1'			4.8	200°
5Z	71°3.7'	157°41.7'			6.3	002°
6A	71°4.8'	157°43.0'			9.9	034°
6B	71°8.2'	157°47.2'			13.0	064°
6C	71°12.8'	157°52.8'			10.8	090°
6D	71°18.3'	157°55.9'			16.2	093°
6E	71°16.2'	157°57.7'			17.4	390°
6F	71°18.9'	158°1.6'			11.8	189°
6G	71°29.3'	158°8.1'				
6H	71°30.7'	158°17.1'	15 Aug			

Position

Sto. ID.	Latitude	Longitude	Date	Time	Speed (cm/sec)	Heading (°T)
27K	71°33.5'	158°15.4'	15 Aug			
27H	71°26.3'	158°6.4'	15 Aug		L08 .1	250°
27G	71°24.4'	158°4.0'	15 Aug		51.9	251°
27F	71°23.4'	158°2.9'	15 Aug		23.8	234°
29A	71°11.5'	157°3.7'	16 Aug	L650	34.2	041°
29B	71°13.1'	157°9.9'		L704	11.7	036" "
29C	71°16.3' -	157°22.0'		L710	60.4	059°
29D	71°18.4'	157°29.8'		L720	56.1	078"
29E	71°19.5'	157°34.5'		L734	74.5	061°
29F	71°25.9'	158°'0.0'		L744	29.1	295°-
29G	71°27.5'	158°5.6'		L 7 5 2	15.8	294"
30D	71°30.5'	157°24.1'		L814	5.8	189°
30D	71°30.51	157°24.1'		1815	5.5	185°
30C	71°27.8'	157°13.0'		L820	9.8	084° - -
30B	71°21.6'	156°49.5'		1855	87.0	054°
30A	71°20.8'	156°46.8'		L907	75.6	052"
1B	71°25.1'	156°34.2'		1943	156.7	045°
1C	71°28.1'	156°34.2'		2006	84.1	041°
1D	71°29.1'	156°34.2'		2017	17.3	045°
1E	71°32.1'	156°34.2'	16 Aug	2 0 2 4	46.7	070°
2A	71°15.7'	156°6.6'	17 Aug	1620	22.7	151°
2P	71°23.7'	156°6.6'	17 Aug	1635	12.2	040°
2C	71°24.7'	156°6.6'	17 Aug	L642	25.3	055°
2D	71°26.7'	156°6.6'	17 Aug	1649	113.8	079°
2E	71°31.7'	156°6.6'	L7 Aug	.838	48.2	087°
2F	71°33.7'	165°6.6'	17 Aug	L846	36.3	093°

Position

Sw ID	Latitude	Longitude	Date	Time	Speed (cm/sec)	Heading (°T)
2G	71°39.7'	156°6.6'	17Aug	1900 "	49.7	228"
2H	71°41.7'	155°54.6'		1911	21.9	204°
3G	71°3507'	155°54.6'		1921	66.9	059°
3F	71°32.7'	155°54.6'		1930	122.8	0 5 1 °
3E	71°27.7'	155°54.6'		1940	23.7	313°
3D	71°24.7'	155°54.6'		1945 -	"20.9 "	329°
3C	71°22.7'	155°54.6'		1953	34.7	309°
33	71°17.7'	1155°54.6'		1958	9.8	238°
3A	71°13.7'	1155°54.6'	17 Aug	2014	22.1	207° "
3	71°28.0'	155°42.6'	19 Aug	1758	81.7	086°
4?	71°23.0'	155°42.6'		1806	9.3	354°
4E	71°17.0'	155°42.6'		1821	14.7	279°
4D	71°16.0'	155°42.6'		1828	13.7	274°
4 D	73°16.0'	155°42.6'		1834	1 1 . 8	274°-
4C	71°15.0'	155°42.6'		1845	2 9 . 1	230°
4B	71°13.0'	155°42.6'	19 Aug	1855	20.4	2 7 3 °
4A	71°12.0'	155°42.6'	19 Aug	1900	20.5	295°
8E	71°5.0'	152°35.4'	20 Aug	L145	12.1	037°
8D	71°4.0'	152°35.4'		L153	9 . 5	018°
8C	70°59.0'	152°35.4'		L201	17.5	016°
8B	70°57.0'	152°47.4'		L208	11.7	358"
8A	70°54.0'	152°35.4'		L217	26.9	359"
9A	70°39.4'	152°6.6'		L242	12.6	041°
9B	70°50.4'	152°6.6'		L301	9.2	329°
9C	70°54.4'	152°6.6'		1.312	6.0	350°
9J	70°55.4'	152°6.6'	20Aug	131.7	14.5	036°

